Optimization of plasmon nano-focusing in tapered metal rods

Michael W. Vogel and Dmitri K. Gramotnev

Applied Optics and Nanotechnology Program, School of Physical and Chemical Sciences, Queensland University of Technology, GPO Box 2434, Brisbane, QLD 4001, Australia.
d.gramotnev@qut.edu.au

Abstract. Analysis of adiabatic and non-adiabatic nano-focusing in tapered metal nano-rods leads to the determination of optimal taper angles and rod lengths as functions of material parameters (for gold, silver, and aluminum) at frequencies from the optical and near infra-red ranges. The considered nano-focusing structures appear to be highly tolerant to such structural and fabrication imperfections as variations of length of the rod and taper angle around their optimal values. However, the major parameter that tends to significantly affect the nano-focusing capabilities of the rods is the radius of the tip, and this is the parameter that should be carefully reproduced in the experiments. Comparison of the numerical results with the adiabatic theory of nano-focusing for different metals and different wavelengths demonstrates the validity of the adiabatic theory in a much wider range of taper angles (up to tens of degrees) than it was previously expected. Major predicted local field enhancements of up to ~ 2,500 times in the considered structures within nano-scale regions as small as a few nanometers will make tapered metal rods highly promising for single molecule detection and development of a new generation of sensors, measurement and nano-manipulation techniques.

Keywords: Surface plasmons, nano-focusing, local field enhancement, near-field optics.

1 INTRODUCTION

Guiding and effective concentration of electromagnetic energy to nano-scale regions is one of the major challenges in nano-optics and nano-photonics [1-22]. This is particularly important for the near field microscopy and spectroscopy with nano-scale resolution, electromagnetic probing of single molecules and quantum dots, non-linear plasmonics, efficient coupling of light into and out of nano-optical circuits and devices, etc. One of the present solutions of this problem is related to using plasmon nano-focusing in metal nano-structures [1-22]. These include dielectric conical tips covered in metal film [1-8], sharply tapered metal rods [11-16], nano-particle lenses [9,10], sharp V-grooves, nano-wedges [17-23], and tapered section of a metal film [24].

One of the most common structures applied for effective plasmon nano-focusing are sharply tapered metal nano-rods [11-16]. This is because such rods provide significantly stronger local field enhancement compared to the other considered nano-focusing structures, especially when dissipation is weak [12,21]. The idea of plasmon nano-focusing in tapered metal rods was first proposed in [11]. The theoretical analysis of plasmon nano-focusing in metal rods is based upon the approximate solution of the wave equation [11] (though applicability conditions for this approach are fairly restrictive), adiabatic approximation (with significantly less restrictive applicability conditions) [12,13], and rigorous numerical analysis based upon the finite-element approach (using the commercially available COMSOL© software package) [14,15]. The experimental investigation of plasmon nano-focusing in a tapered metal rod, as an effective nano-scale broadband light source, was conducted in Ref. 16.

Issa and Guckenberger [14] reported the rigorous numerical analysis of non-adiabatic plasmon nano-focusing in metal rods with rounded tips and arbitrary taper angles. The obtained results included several important features one of which is the existence of an

Received 7 Aug 2008; accepted 19 Nov 2008; published 21 Nov 2008 [CCC: 19342608/2008/$25.00]
Journal of Nanophotonics, Vol. 2, 021852 (2008)

optimal taper angle of the rod (similar results were obtained for tapered nano-gaps [18,21]) for achieving strong local field enhancement at the tip [14]. The dependence of this optimal taper angle on wavelength has also been investigated, demonstrating a significant decrease of the optimal angle, together with the simultaneous increase of the local field enhancement at the tip, when plasmon frequency is decreased [14]. It was also shown that increasing length of the tapered rod, while keeping taper angle constant, also resulted in increasing local field enhancement at the tip (while the optimal taper angle did not seem to depend noticeably on length of the nano-focusing rod) [14].

The comparison of the rigorous numerical results with the adiabatic theory based on the geometric optics approximation [26] led to the conclusion that the approximate adiabatic theory remains applicable up to the values of the adiabatic parameter $\delta = \partial(Q_1^{-1})/\partial z \sim 1$ (instead of $\delta << 1$, as was suggested previously [12,13,17]), where Q_1 is the real part of the plasmon wave number, and the z-axis is parallel to the axis of the conical rod and the direction of plasmon propagation. However, this conclusion has so far been made based on the analysis of only plasmons in gold rods at the vacuum wavelength $\lambda_{vac} =$ 632.8 nm (He-Ne laser) [26]. Whether it will stand for other wavelengths and metals is still an open question. Similarly, it is not entirely clear if it is possible to use the simple adiabatic theory to determine optimal taper angles, and how to use the adiabatic results to evaluate the local field enhancement at the rounded tip of the tapered rod in the presence of plasmon reflections from the tip.

Further rigorous numerical analysis of non-adiabatic nano-focusing in tapered rods also demonstrated the existence of an optimal length of the tapered rod, at which the local field enhancement at the rounded tip is maximal [26]. A simple analytical equation for the optimal length of the tapered rod was derived [26]. This was done on the basis of the understanding that the optimal length of the tapered rod corresponds to the distance from the tip, at which the increase in the plasmon amplitude due to the focusing effect of the tapered rod is exactly compensated by the decrease of the plasmon amplitude due to its dissipation in the metal [26]. In particular, these results allowed the determination of the optimal structural parameters for nano-focusing gold rods. However, the dependence of the optimized parameters of tapered rods on plasmon wavelength and different material parameters has not been investigated so far.

Therefore the aim of this paper is to report the detailed numerical investigation of plasmon nano-focusing in tapered metal rods of different material and structural parameters at different plasmonic wavelengths. Optimization of structural and material parameters will be conducted for the considered nano-focusing rods with the aim of achieving maximum possible field enhancement of the rounded tip of different radii. This will include the determination of the optimal taper angles and lengths of the rods, and their dependencies on material parameters. Generalization of the applicability conditions for the adiabatic theory of plasmon nano-focusing will be carried out for conical rods made of different metals. It will also be demonstrated that for major types of metals and plasmon wavelengths the optimal structural parameters can reasonably be evaluated from the simplified adiabatic theory of nano-focusing. Correction factors will be introduced and analyzed enabling the use of the adiabatic theory to determine the local field enhancement at the rounded tip in the presence of plasmon reflections from the tip. In addition, the numerical analysis of the field structure at the rounded tip of the rod will also be carried out, revealing noticeable differences for different types of metal, which may be useful for applications in near-field microscopy and spectroscopy with nano-scale resolution.

2 STRUCTURE AND METHODS OF ANALYSIS

The analyzed structure is presented in Fig. 1a. A metal tapered rod with a taper angle α and complex permittivity $\varepsilon_m = e_1 + ie_2$ ($e_1 < 0$, $e_2 > 0$) is surrounded by a lossless dielectric medium with a permittivity ε_d (we limit our consideration to the case where the tapered rod is surrounded by vacuum, i.e. $\varepsilon_d = 1$). The coordinate axes are as shown in Fig. 1a. The analysis will be conducted for a TM (transverse magnetic) plasmon mode with

the magnetic field having only φ-component. Both the electric and magnetic fields are independent of the angle φ. Only such TM plasmons can exist at arbitrarily small rod diameters and thus experience nano-focusing in a tapered rod [12,13].

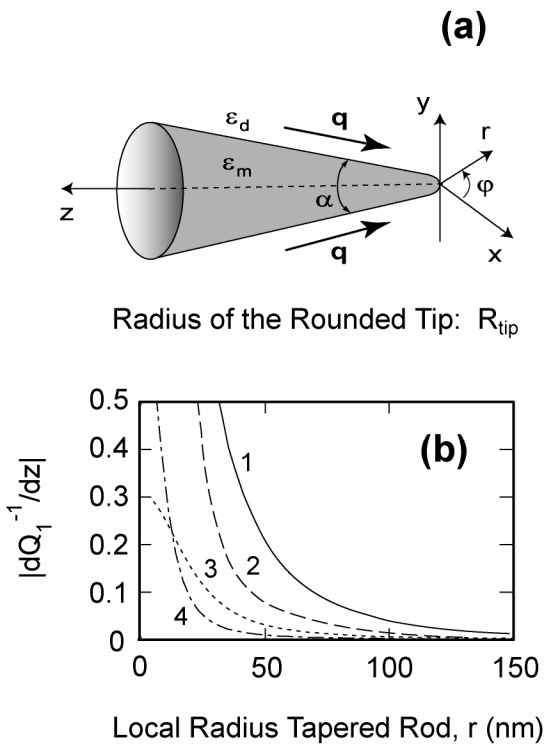

Fig. 1. (a) A metal rod with the taper angle α, permittivity $\varepsilon_m = e_1 + ie_2$, and rounded tip of radius R_{tip}, surrounded by a lossless dielectric material with the real and positive permittivity ε_d, **q** is the wave vector of the TM surface plasmon propagating towards the tip of the rod, (x,y,z) and (r,φ,z) are the Cartesian and cylindrical systems of coordinates. (b) The dependencies of the adiabatic parameter δ (the left-hand side of inequality (1)) on local radius of the tapered rod for the same vacuum wavelength λ_{vac} = 632.8 nm (He-Ne laser) but different metals and taper angles: (1) Aluminum (ε_m = – 55.909 +22.017i [23]), α = 10°, (2) Aluminum, α = 50°, (3) Gold (ε_m = – 11.44 +1.12i [23]), α = 10° and (4) Silver (ε_m = – 16.102 +1.076i [23]), α = 50°. Q_1 is the real part of the plasmon wave number q in the rod.

If the taper angle of the rod is sufficiently small, so that the variations of the plasmon wave number within one plasmon wavelength are negligible at all distances from the tip of the rod, then the adiabatic approximation (geometrical optics approximation) can be applied for the analysis of nano-focusing. Mathematically, the applicability condition for the adiabatic approximation can be written as [12,13,16,18]:

$$\delta = \left| \frac{d(Q_1)^{-1}}{dz} \right| << 1 \qquad (1)$$

where δ is the adiabatic parameter, Q_1 is the real part of the plasmon wave number $q = Q_1 + iQ_2$ in the tapered rod as a function of the local rod diameter, and plasmon dissipation is assumed to be weak: $Q_2 << Q_1$. However, the previous numerical analysis conducted in [21,22,26] demonstrated that this inequality appears excessively restrictive, and the adiabatic theory is applicable for gold rods if [26]

$$\delta \le 0.85, \qquad (2)$$

which is thus the actual applicability condition for the approximate adiabatic theory.

Figure 1b presents the dependencies of the adiabatic parameter δ on local radius of gold, silver and aluminum tapered rods in vacuum ($\varepsilon_d = 1$) for the vacuum wavelength $\lambda_{vac} = 632.8$ nm ($\varepsilon_m = -11.44 + 1.12i$ for gold, $\varepsilon_m = -16.102 + 1.076i$ for silver, and $\varepsilon_m = -55.909 + 22.017i$ for aluminum [25]) and different taper angles. From Fig. 1b it can be seen that if the taper angle α is large, then inequality (2) may be breached near the tip (curves 1, 2 and 4 in Fig. 1b), while sufficiently far from the tip, where the rod diameter is larger than the plasmon wavelength, it is satisfied at all taper angles (Fig. 1b). This is because the plasmon wave number starts to vary significantly (at large α) with reducing rod diameter only when this diameter becomes smaller than the plasmon wavelength. Therefore, the adiabatic approximation is applicable for the analysis of plasmon propagation sufficiently far from the tip of the rod practically at all taper angles. It is only near the tip (at small local radii) that condition (2) may restrict the applicability of the adiabatic theory.

Therefore, in this paper, we will use the approach that was previously developed in Ref. 26, which is a combination of the adiabatic theory for plasmon propagation in a tapered rod at relatively large distances from the tip (where condition (2) is satisfied), and the rigorous numerical theory based on the finite element analysis (COMSOL software package) in the vicinity of the tip (where condition (2) is breached). Such a combination of the two approximate and rigorous methods is convenient for accurate analysis of plasmon nano-focusing in rods up to tens of microns (or more) in length and arbitrary taper angles, which is impossible or could be difficult (due to limited computational resources) in either of the mentioned methods separately [26]. The analysis of such long rods is important, because, as has been shown in Ref. 26, the optimal length of the rod (resulting in the maximum possible local field enhancement at the tip of the rod) is about ~ 10 μm (for gold at $\lambda_{vac} = 632.8$ nm). Some other materials, e.g., silver, could be expected to correspond to even larger optimal rod lengths. For the detailed discussion of the approach based on the combination of the rigorous and adiabatic theories see Ref. 26.

Figure 1b demonstrates that at the considered vacuum wavelength $\lambda_{vac} = 632.8$ nm, for all metal tapered rods with taper angles as large as $\alpha = 50^o$, even more restrictive condition (1) is satisfied for local rod diameters $2r \gtrsim 200$ nm (r is the local radius of the rod). In accordance with this, we use the rigorous finite element analysis for the tapered section of the rod between the rounded tip and the local radius $r = 300$ nm, and the adiabatic theory for the remaining section of the rod with $r > 300$ nm (similar to how it was done in Ref. 26). The results obtained from both the approaches are then matched at $r \approx 300$ nm, i.e., the amplitude of the plasmon incident onto the tip in the numerical approach at the local radius $r \approx 300$ nm is made equal to the amplitude of the plasmon obtained from the adiabatic theory at the same local radius [26].

A TM plasmon incident onto the rounded tip of the tapered rod (Fig. 1a) experiences reflection from this tip, because the adiabatic conditions (1) and (2) are not satisfied at the rounded tip, no matter how small the taper angle is. The reflected plasmon forms an interference standing wave pattern with the incident plasmon traveling towards the tip [26]. In addition, the plasmon reflected from the rounded tip and traveling in the positive z-direction (Fig. 1a) may also experience reflections from the point of the "end-fire excitation," where the incident plasmon field is introduced in COMSOL at $r = 300$ nm. As a result, significant Fabry-Perot effect may occur in the finite element analysis between the rounded tip and the point of the end-fire excitation in the rigorous analysis [26]. At the same time, these multiple reflections in the rigorous analysis are rather not real, as they occur due to plasmon reflections from the point of the end-fire excitation (at $r = 300$ nm) with non-physical artificial boundary conditions that specify the field of the incident plasmon in the considered section of the rod. Therefore, a normalization procedure has been developed in Ref. 26 to eliminate this artificial Fabry-Perot effect, during which the local field at the tip is normalized to the amplitude of the incident plasmon in the artificial Fabry-Perot cavity (i.e., near the point of the end-fire excitation at $r \approx 300$ nm) – see Ref. 26 for more detail. The same procedure is also used in this paper for further analysis and

optimization of plasmon nano-focusing in tapered rods made of different metals and at different plasmon wavelengths.

3 RESULTS AND DISCUSSIONS

Figure 2a shows the dependencies of the local electric field enhancement at the rounded tip (with the radius of curvature of the tip R_{tip} = 2 nm) at the optimal taper angle on length L of the tapered section of the rod for the silver rod (curve 1; and the optimal taper angle $\alpha_{opt} \approx 30^o$), gold rod (curve 2; $\alpha_{opt} \approx 37^o$), and aluminum rod (curve 3; $\alpha_{opt} \approx 20^o$). It can be seen that for all three metals there is an optimal length of the rod L_{opt} that results to the maximal possible local field enhancement at the rounded tip (see also Ref. 26). However, it is also seen that these optimal lengths may be quite different for different metals (Fig. 2a). For example, for silver this optimal length is ~ 22 μm, while for gold and aluminum it is ~ 10 μm and ~ 14 μm, respectively. All three optimal lengths are in excellent agreement with the approximate analytical equation for L_{opt} derived previously in Ref. 26:

$$L_{opt} \approx \frac{e_1(\varepsilon_d + e_1)}{e_2 \varepsilon_d q_0} \cos(\alpha/2). \tag{3}$$

Here, q_0 is the wave number of the surface plasmon on the flat metal interface (i.e., when $r = +\infty$). Note that, as also derived in [26], this simple equation is correct only for relatively large taper angles, such that

$$\sin(\alpha/2) >> \frac{e_2 \varepsilon_d}{e_1(\varepsilon_d + e_1)}. \tag{4}$$

In accordance with Eq. (3), the optimal rod length does not depend on radius of the rounded tip, but does depend upon plasmon frequency (wavelength), because q_0, e_1 and e_2 are frequency-dependent. This means that the curve maxima seen in Fig. 2a are achieved at the same rod lengths, irrespectively of radius of the tip. In addition, because the maxima displayed by the curves in Fig. 2a are relatively broad for all the metals, it can also be said that fluctuations of the rod length around its optimal value (for example, due to fabrication imperfections) do not have a major impact on the nano-focusing capabilities of the rods. For example, varying length of an aluminum rod between ~ 10 μm and ~ 30 μm does not have a noticeable impact on the maximal local field enhancement at the tip (see curve 3 in Fig. 2b). Therefore, Eq. (3) provides an excellent guide for the determination of optimal rod lengths for a range of taper angles, metals, and other material parameters.

It is also important to note the significant differences in the values of the local field enhancement achievable by means of using different metals (compare the curves in Fig. 2a). These differences are predominantly related to the different levels of dissipation in the considered metals. The strongest dissipation in aluminum results in the lowest local field enhancement at the rounded tip. Nevertheless, even for aluminum, very strong local field enhancement of more than ~ 500 times can be achieved (curve 3 in Fig. 2a). The local field enhancement for gold and silver (of ~ 1600 times and ~ 2400 times, respectively) clearly demonstrate the remarkable potential of plasmon nano-focusing in tapered rods for achieving single molecule detection by means of surface-enhanced Raman spectroscopy. Indeed, such detection should require enhancement of Raman signal by a factor of ~ 10^{13} – 10^{14}. Taking into account that Raman signal is proportional to the fourth power of the local electric field, we can see that the required Raman enhancements could be achievable in the considered nano-focusing structures (for silver and gold).

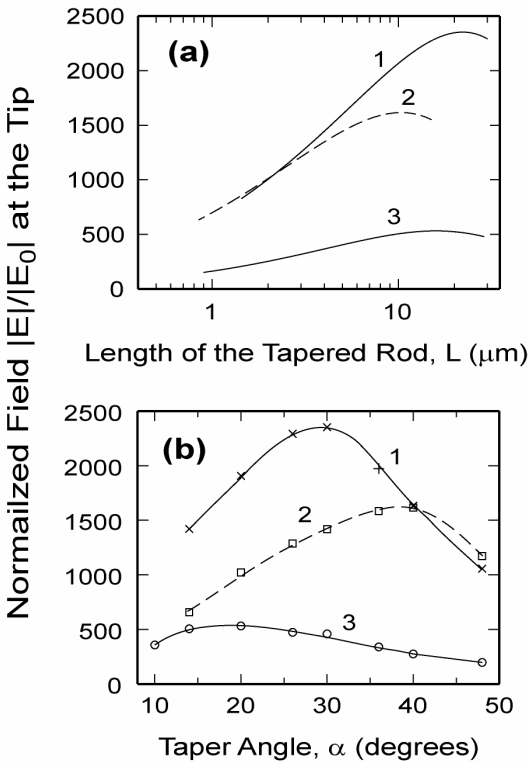

Fig. 2. (a) The dependencies of the local electric field enhancement at the rounded (with the radius of curvature R_{tip}= 2 nm) tip of the tapered silver (curve 1; ε_m = – 16.102 +1.076*i* [25]), gold (curve 2; ε_m = – 11.44 +1.12*i* [25]) and aluminum (curve 3; ε_m = – 55.909 +22.017*i* [25]) rods on rod length L at the optimal taper angle $\alpha = \alpha_{opt} \approx 30^o$, 37^o, and 20^o for silver, gold, and aluminum, respectively, λ_{vac} = 632.8 nm (He-Ne laser), and ε_d = 1. The local electric field $|E|$ at the tip (i.e., at $z = 0$) is normalized to the amplitude of electric field $|E_0|$ in the plasmon at the initial cross-section of the rod at $z = L$. This is equivalent to having $|E_0| = 1$ at $z = L$ (where $r = r_0$). (b) The dependencies of the local electric field enhancements at the rounded tip of the tapered silver (curve 1), gold (curve 2) and aluminum (curve 3) rods on taper angle α at the optimal rod length $L = L_{opt}$ obtained from (a) or Eq. (3).

As mentioned above, the optimal rod length depends only weakly on taper angle α. For example, changing taper angle between 10^o and 50^o for the considered silver, gold and aluminum rods does not result in any notable variations of L_{opt}. Therefore, Fig. 2b presents the dependencies of the local field enhancement at the rounded tip on taper angle α for the optimal rod lengths $L = L_{opt}$ (which is approximately independent of taper angle) for the considered metal rods. Curves 1 – 3 in Fig. 2b correspond to the silver, gold and aluminum rods, respectively.

The curves in Fig. 2b confirm the existence of the optimal taper angles for different metals, and demonstrate their dependence on metal permittivity. For example, gold corresponds to the largest optimal taper angle, whereas the optimal taper angle for aluminum is the smallest. This is because the magnitude of the dielectric permittivity for gold is the smallest. Therefore, the plasmon wavelength for gold is also the smallest, which means that the applicability conditions for the adiabatic approximation (Eqs. (1) and (2)) are satisfied at larger taper angles. Indeed, smaller wavelength corresponds to smaller variations of the rod radius within this wavelength, and thus smaller variations of the plasmon wave number within one plasmon wavelength (see Eqs. (1) and (2)). As a result, plasmon reflections from the taper (and thus the reflective losses of the plasmon energy) in gold rods become significant at noticeably larger taper angles than for aluminum (whose per-

mittivity is the largest). This leads to larger optimal taper angles for gold, because these angles correspond to significant reflective losses of plasmon energy (see also Ref. 26).

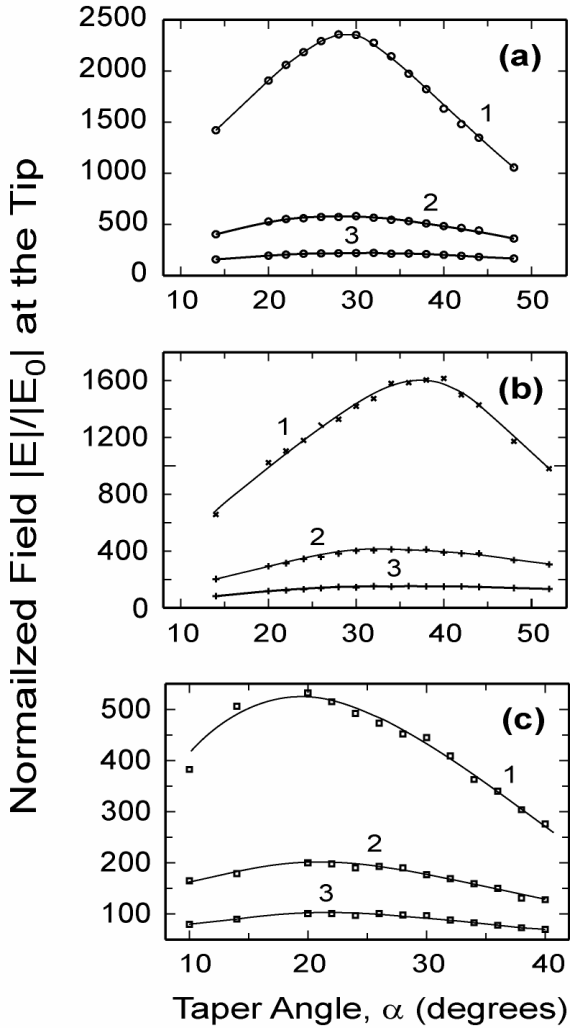

Fig. 3. The dependencies of the local field enhancement at the rounded tip on taper angle of the rod for different metals: (a) silver, (b) gold, (c) aluminum, and at different radii of curvature of the tip: R_{tip} = 2 nm (curves 1 – the same as the three curves in Fig. 2a), 5 nm (curves 2), and 10 nm (curves 3). The length of the rod $L = L_{opt}$, $\varepsilon_d = 1$, λ_{vac} = 632.8 nm (He-Ne laser). The normalization of the local electric field $|E|$ at the tip (i.e., at $z = 0$) is conducted to the initial amplitude of electric field $|E_0|$ in the plasmon at $z = L_{opt}$.

It is also important to note that the sensitivity of the nano-focusing capabilities of the tapered rods to relatively small variations of the taper angle (around the optimal angle αopt) is low. For example, for silver rods, varying taper angle between ~ 25^o and ~ 35^o does not lead to major variations in the local field enhancement at the rounded tip (curve 1 in Fig. 2b). Similarly, for aluminum rods, varying taper angle even in the larger range between ~ 10^o and ~ 30^o results in almost constant local field enhancement at the tip (curve 3 in Fig. 2b). This demonstrates high tolerance of the tapered rod nano-focusing structures to significant structural imperfections of such parameters as taper angle and rod length. This is a significant aspect that will be important for practical observations and applications of plasmon nano-focusing in nanophotonics, and fabrication of the respective structures. Another practical simplification for observation and use of plasmon nano-

focusing in tapered rods is related to the fact that optimal lengths are relatively large, i.e. typically ~ 10 μm or more. This may be seen as another benefit for practical fabrication of such structures.

It is also important to understand the physical differences for the existence of the optimal rod length L_{opt} and the optimal taper angle α_{opt}. The optimal length of the rod L_{opt} is equal to the distance from the rounded tip, at which the focusing effect of the tapered rod (as the plasmon propagates towards the tip trough progressively reducing cross-sections of the rod) is exactly cancelled by plasmon dissipation [26]. On the other hand, at the optimal taper angle α_{opt}, the tendency of increasing focusing effect in the rod with increasing its taper angle is cancelled by the opposite tendency of increasing reflective losses of the plasmon energy from the taper due to the increased non-adiabaticity [18,21,26].

The effect of different radii R_{tip} of the rounded tip of the tapered rod on the local enhancement of the electric field at the tip is demonstrated by Fig. 3 for the three considered metals: silver (Fig. 3a), gold (Fig. 3b), and aluminum (Fig. 3c). A major result is that the local field enhancement at the tip rapidly increases with decreasing its radius of curvature R_{tip}. For example, decreasing R_{tip} from 5 nm to 2 nm results in ~ 5 times increase of the local electric field enhancement for silver (curves 1 and 2 in Fig. 3a), ~ 4 times for gold (curves 1 and 2 in Fig. 3b) and ~ 3 times for aluminum (curves 1 and 2 in Fig. 3c). This demonstrates the high sensitivity of the rod nano-focusing structures to radius of the tip for all metals. Therefore, careful fabrication of the rounded tip of the tapered rod is crucial for achieving repeatable and controllable local field enhancements. On the other hand, the optimal taper angle α_{opt} only very weakly depends on R_{tip} for all the metals. It is possible to notice only very weak tendency towards increasing optimal taper angle with decreasing radii of the tip (Figs. 3a-c).

The minimal radius of the rounded tip R_{tip} = 2 nm has been chosen so that to avoid the effects of spatial dispersion, Landau damping and the atomic structure of matter [12], which is beyond the scope of this paper.

4 ADIABATIC AND NON-ADIABATIC THEORIES

In this section, we compare the adiabatic and non-adiabatic theories of nano-focusing in tapered metal rods and, in particular, determine/verify numerically the applicability conditions for the adiabatic theory (Eqs. (1) and (2)) for the three considered metals. Adiabatic theory assumes no plasmon reflections from the tip of the rod [12,13]. At the same time, rigorous numerical analysis of nano-focusing in tapered rods with rounded tips always results in some plasmon reflection from the tip. The reflected plasmon inevitably contributes to the overall local field in the rod [26]. Therefore, in order to compare the approximate (adiabatic) and rigorous numerical results, we have to eliminate reflections from the tip in the numerical simulation. This can be achieved by removing the rounded tip of the tapered rod and attaching, instead, a uniform nano-wire to the exit cross-section of the rod [26]. The diameter of the nano-wire is the same as that of the smallest (exit) diameter of the tapered rod (Fig. 4a).

The length of the nano-wire is chosen so that the plasmon efficiently dissipates in the nano-wire, and no plasmon reflections from its free end have to be taken into account. In this case, the plasmon will largely continue to propagate from the tapered section of the rod into the wire, rather than being reflected from the exit cross-section of the rod (if the angle α is not too large). Thus there will be no reflected plasmon in the tapered section of the rod, which enables the direct comparison with the adiabatic theory of nano-focusing [12,13].

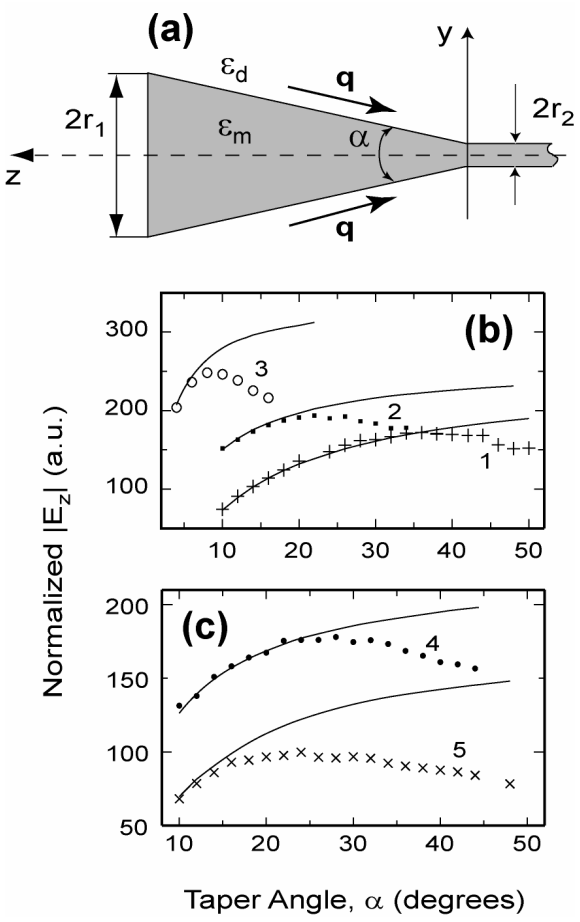

Fig. 4. (a) The structure for the comparison of the adiabatic and non-adiabatic theories of nano-focusing in a tapered metal rod. A uniform metal nano-wire of the same material as the tapered rod is attached to the smallest (exit) cross-section of the rod in order to suppress (reduce) plasmon reflections from the tip. (b, c) The points show the rigorous dependencies of the *z*-component of the electric field in the focused TM plasmon in vacuum near the metal surface at the smallest (exit) cross-section of radius $r = r_2$ of the tapered section of the metal rod on taper angle α; $\varepsilon_d = 1$, $r_1 = 300$ nm, $r_2 = 5$ nm. (1) Gold, $\lambda_{vac} = 632.8$ nm, $\varepsilon_m = -11.44 + 1.12i$ [25], (2) Gold, $\lambda_{vac} = 780$ nm, $\varepsilon_m = -21.214 + 1.724i$ [25], (3) Gold, $\lambda_{vac} = 1600$ nm, $\varepsilon_m = -102.66 + 11.964i$ [25], (4) Silver, $\lambda_{vac} = 632.8$ nm, $\varepsilon_m = -16.102 + 1.076i$ [25], and (5) Aluminum, $\lambda_{vac} = 632.8$ nm, $\varepsilon_m = -55.909 + 22.017i$ [25]. The solid curves represent the respective dependencies obtained from the adiabatic theory [12,13].

This comparison is demonstrated by the curves in Figs. 4b,c for the three considered metals. As can be seen from Figs. 4b,c, for all considered metals and plasmon frequencies, there is a general tendency for the rigorous curves to closely follow the approximate adiabatic solution at relatively small taper angles. However, at some larger values of the angle α, there appear significant deviations of the rigorous curves from the adiabatic dependencies. All the rigorous curves go through maxima and then start to decrease monotonically. This is very similar to what was also observed in Ref. 26 for gold tips at the wavelength $\lambda_{vac} = 632.8$ nm. It is clear that increasing plasmon wavelength results in significant changes (reduction) of the taper angle at which the discrepancies between the approximate (adiabatic) and rigorous theories start to appear – compare rigorous curves 1 – 3 in Fig. 4b. The reason for this is the same as for increasing optimal taper angle with increasing magnitude of the metal permittivity, which was explained above in discussions

of the curves in Fig. 2b (increasing wavelength results in increasing magnitude of the metal permittivity [25]).

It was indicated in Sec. 2 and shown in Ref. 26, that the adiabatic approximation for a gold tapered rod at the wavelength λ_{vac} = 632.8 nm is valid if condition (2) is satisfied (contrary to the more conventional assumption that more restrictive condition (1) should be satisfied). It is important to verify this finding for different metals and plasmon wavelengths (which means different material parameters of the nano-focusing structure).

The critical taper angle α_c for a tapered rod can be defined as the angle at which the results obtained in the adiabatic theory and non-adiabatic rigorous calculation start to diverge significantly (Figs. 4b, c). The critical angles for a gold tapered rod at λ_{vac} = 632.8 nm, 780 nm, and 1600 nm are $\alpha_c \sim 40^o$, 25^o, and 13^o, respectively (Fig. 4b). For a silver and aluminum tapered rods at λ_{vac} = 632.8 nm, $\alpha_c \sim 30^o$ and $15^o - 20^o$, respectively (curves 4 and 5 in Fig. 4c). Above these critical angles, reflections of the plasmon from the taper itself appear to be strong enough to noticeably reduce the overall energy reaching the exit cross-section at $z = 0$ (Fig. 4a), and this results in decreasing local field enhancement at $z = 0$ in the rigorous numerical analysis, compared to the adiabatic theory. This explains the significant deviations of the numerical curves from those obtained in the adiabatic approximation for larger taper angles $\alpha > \alpha_c$ (Figs. 4b,c).

It is important to note that all the rigorous curves in Figs. 4b,c start to significantly deviate from the adiabatic curves when the adiabatic parameter δ becomes larger than ~ 0.85. Therefore, it appears that the value of the adiabatic parameter $\delta \approx 0.85$ is a fairly universal and reliably determines the applicability conditions for the adiabatic theory for rod nano-focusing structures with different metals and at different plasmon wavelengths. This is the reason why it has appeared in inequality (2).

As explained above, the discrepancies between the rigorous and adiabatic theories appear when plasmon reflections from the taper, due to non-adiabaticity, start to cause significant energy losses in the propagating plasmon. On the other hand, the same physical effect results in the existence of an optimal taper angle α_{opt} that corresponds to a maximum of the local field enhancement at the rounded tip of the rod. Therefore, it could be expected that the optimal taper angle could be evaluated using the adiabatic theory by simply calculating the taper angle at which the adiabatic parameter $\delta \approx 0.85$.

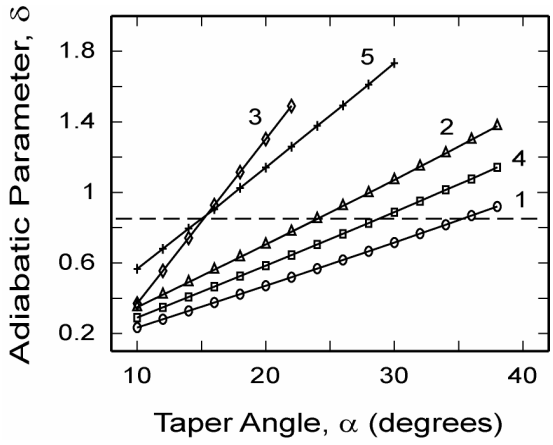

Fig. 5. The dependencies of the adiabatic parameter δ on taper angle at the smallest (exit) cross-section of the tapered rod of radius $r = r_2$ for the structure presented in Fig. 4a. The structural and material parameters are the same as for Fig. 4. The numbers of the curves corresponds to those in Figs. 4b,c.

Figure 5 shows the dependencies of the adiabatic parameter δ on taper angle for gold, silver and aluminum tapered rods at the vacuum wavelengths λ_{vac} = 632.8 nm, 780 nm and 1600 nm. The dashed horizontal line corresponds to the adiabatic parameter $\delta = 0.85$.

The angles determined by the intersection points with the horizontal dashed line corresponding to the adiabatic parameters $\delta = 0.85$ (Fig. 5) could be taken as a definition of the critical taper angles α_c. As expected, these angles are very close to the previously determined optimal taper angles α_{opt} resulting in the maximum local field enhancement at the rounded tip (Fig. 3). There is a slight discrepancy between $\alpha_{opt} \sim 20^o$ (Fig. 3c) and $\alpha_c \sim 15^o$ (Fig. 5) for aluminum rods. However, because of the significant width of the enhancement maximum near the optimal taper angle (Fig. 3c), this discrepancy is of no practical importance, and the critical angle obtained from Fig. 5 could also be regarded as a good approximation for α_{opt}. Thus, the applicability condition for the adiabatic approximation (2) can simultaneously be used for the approximate determination of the optimal taper angle of a tapered nano-focusing metal rod in a wide range of material parameters and wavelengths.

It is also interesting to note that, for example, for silver rods, the adiabatic theory appears to be valid up to angles $\sim 30^o$, and these angles appear to be significantly larger than those for a tapered groove ($\sim 16^o$ [18,21]). At this stage, a physical explanation of this difference is not fully understood, but it should be related to weaker reflections of the plasmon in a tapered rod compared to a tapered groove.

As mentioned in the beginning of this section, the plasmon reflected from a rounded tip of a tapered rod significantly affects the typical local field enhancement. This effect cannot be accurately considered in the adiabatic approximation, as this approximation is breached at the rounded tip. As a result, the local field enhancements obtained in the adiabatic theory (with no reflected plasmon) can be significantly underestimated. Therefore, correcting factors can be introduced to enable more accurate use of the approximate adiabatic theory for the evaluation of the typical local field enhancements at a rounded tip of a tapered metal rod. Because of the rotational symmetry of the charge distribution in the TM plasmon propagating in a tapered rod (the charge density in the rod is independent of the φ-coordinate), the incident localized plasmon will hardly radiate any bulk waves upon its reflection from the rounded tip with sufficiently small radius – there will be no dipole radiation in this case [27]. Therefore, practically all the energy of the incident plasmon is reflected back from the rounded tip. On the other hand, the uniform dielectric medium beyond the rounded tip (at $z < 0$ – Fig. 1a) can be regarded as the dielectric medium with an infinitely thin rod (with $r = 0$). The speed of the TM plasmon with the considered field symmetry in such a rod with the zero radius (at $z < 0$) must also be zero. It can thus be said that when the plasmon is reflected from a rounded tip, it is actually reflected from an interface with the effective medium (at $z < 0$) in which the plasmon speed is zero. In this case, the standing wave pattern in the rod formed by the incident and reflected plasmons must have an anti-node at the interface, i.e., at $z = 0$, similar to a wave in a string with a free end. Therefore, the typical local field enhancement at the rounded tip is expected to be ~ 2 times larger than that obtained in the adiabatic theory with no reflections of the plasmon from the tip.

Figure 6 presents the dependencies of the ratio of the local field amplitude of the plasmon at the apex of the rounded tip (Fig. 1a), obtained in the rigorous numerical analysis, to the amplitude of the field at the surface of the tapered rod at the smallest (exit) cross-section of radius $r = r_2$ for the structure presented in Fig. 4a, obtained in the adiabatic theory. It can be seen that the typical values of this ratio at not very large taper angles is between 2 and 3 for the three considered metals (gold, silver, and aluminum). All the three curves display monotonic decrease with increasing taper angle. Curves 1 and 2 for gold and silver display the tendency to plateau at small taper angles that are below the optimal angle α_{opt}.

Such a behavior of the dependencies in Fig. 6 is expected. Firstly, the monotonic decay of the displayed dependencies in Fig. 6 with increasing taper angle is related to increased reflections of the plasmon from the taper itself, which results in decreasing local field at the apex of the tip in the rigorous numerical theory at $\alpha > \alpha_{opt}$. As a result, the

differences between the local fields obtained in the rigorous and adiabatic theories decrease with increasing taper angle, leading to a monotonic decay of the curves in Fig. 6.

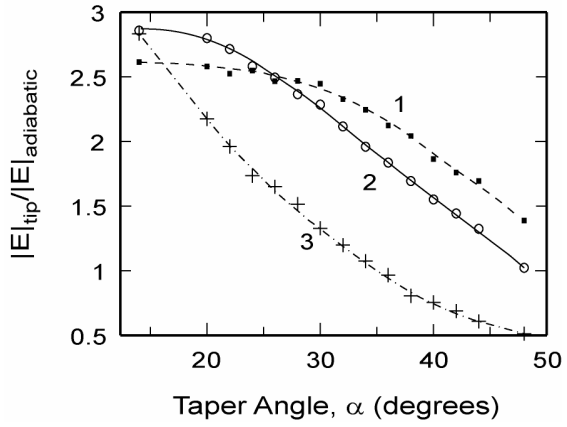

Fig. 6. The dependencies of the ratio of the local field amplitude of the plasmon at the apex of the rounded tip (Fig. 1a), obtained in the rigorous numerical analysis, to the amplitude of the field at the surface of the tapered rod at the smallest (exit) cross-section of radius $r = r_2$ for the structure presented in Fig. 4a, obtained in the adiabatic theory. The dependencies are presented for the vacuum wavelength λ_{vac} = 632.8 nm and three different metals surrounded by vacuum: gold (curve 1), silver (curve 2), and aluminum (curve 3).

Secondly, the existence of the plateaus at $\alpha < \alpha_{opt}$ is explained by the absence of significant reflections of the plasmon from the taper. Therefore, though the local field enhancement does depend on taper angle for both the rigorous and adiabatic theories, this dependence is cancelled out from the ratio of the local fields presented in Fig. 6. The curve for aluminum does not display a plateau in Fig. 6 because for aluminum rod $\alpha_{opt} \sim 15^o$, and the range with $\alpha < \alpha_{opt}$ is not presented in Fig. 6 for this metal.

Thirdly, the typical values of the ratio of the local amplitudes obtained in the rigorous and adiabatic theories at small taper angles $\alpha < \alpha_{opt}$ are larger than the expected 2 times increase caused by the existence of an anti-node of the standing wave pattern created by the incident and reflected plasmons. This discrepancy is explained by the additional sharpness of the rounded tip due its roundness, which leads to further increase of the local field at the apex of the tip.

Thus, Fig. 6 demonstrates that in order to obtain approximate values of the local field enhancement at the apex of a rounded tip of a tapered rod with a taper angle $\alpha \le \alpha_{opt}$, it is necessary to multiply the results obtained in the adiabatic theory by a factor of ~ 2.5 – 3 for all three considered metals.

5 FIELD STRUCTURE AT THE ROUNDED TIP

The important areas of application of plasmon nano-focusing in tapered metal rods are related to near-field microscopy, spectroscopy, trapping and manipulation of very small nano-particles and even separate molecules. From this point of view, an important feature of plasmon nano-focusing is the field structure and localization near the tip of the rod, including typical dimensions of the region of the field localization and field penetration into the surrounding dielectric medium. Therefore, in this section, we will analyze the distribution of the electromagnetic field along the surface of the rounded tip and investigate how this distribution depends upon angle of the tapered rod, its material parameters, and radius of the rounded tip R_{tip}. Actually, we will be interested in the distribution of the electric field, because the magnetic field in metallic nano-focusing structures plays insignificant role because it is much weaker than the electric field [21].

Figure 7a presents the field distributions along the surface of the rounded tip with R_{tip} = 5 nm for the tapered gold and silver rods with the same taper angles $\alpha = 20^o$ (curves 1 and 3, respectively) and $\alpha = 40^o$ (curves 2 and 4, respectively). Fig. 7b presents the field distributions for the tapered gold and aluminum rods with taper angles $\alpha = 20^o$ (curves 1 and 3) and $\alpha = 40^o$ (curves 2 and 4). All the distributions are normalized to the magnitude of the electric field exactly at the rounded tip (where the electric field is maximal).

As can be seen from Figs. 7a,b, the electric field monotonically decays away from the top of the rounded tip along its surface (i.e., with increasing x) for all the materials and taper angles. However, the rate of this decay may be significantly different for different rods. For example, it noticeably increases with increasing taper angle of the rod (compare curves 1 and 2, and 3 and 4 in Figs. 7a,b). This means that increasing taper angle results in increasing localization of the field near the top of the rounded tip (i.e., near $\theta = 0$). This feature may be important for the design of most effective structures manipulation of very small nano-particles (with dimensions of a few nanometers) or even separate molecules by, for example, trapping them in the strongly localized plasmonic field near the top of the rounded tip.

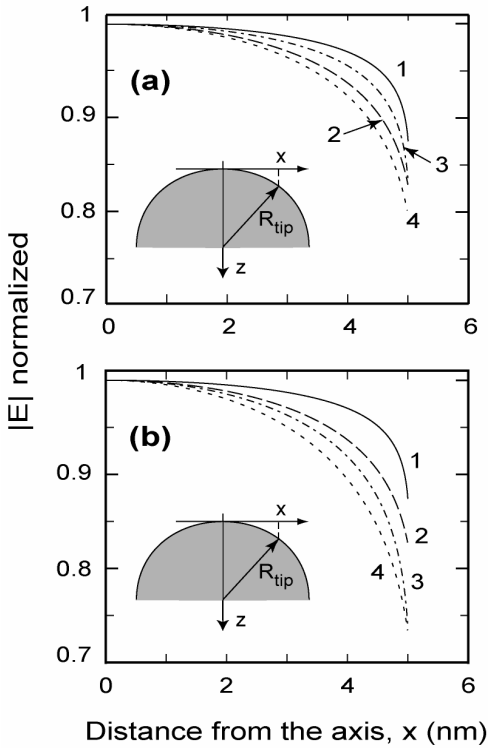

Fig. 7. The typical field distributions of the normalized electric field $|E|$ along the surface of the rounded tip with the radius R_{tip} = 5 nm. (a) Curves 1 and 2: gold rods with taper angles $\alpha = 20^o$ and $\alpha = 40^o$, respectively. Curves 3 and 4: silver rods with the same taper angles $\alpha = 20^o$ and $\alpha = 40^o$, respectively. (b) Curves 1 and 2: the same as for (a). Curves 3 and 4: aluminum rods with the same taper angles $\alpha = 20^o$ and $\alpha = 40^o$, respectively. The insets show the rounded tips with the x-coordinate and θ-angle measured from the top of the rounded tip.

Similarly, for the aluminum rods, the field localization (confinement) near the top of the rounded tip (at $\theta = 0$) appears significantly stronger than for silver and especially gold rods. This follows from the comparison of curves 1 and 3, and 2 and 4 in Fig. 7b, which show significantly larger rates of field decay along the surface of the rounded tip for metals with larger magnitude of the permittivity.

Figure 8 presents the dependencies of the typical distances from the top of the rounded tip, such that at these distances the local electric field is reduced e times. The presented dependencies are on taper angle for three different metals: gold, silver and aluminum. These distances represent the size of the localization region (localization depth) for the plasmonic field near the tip in the z-direction. One of the main outcomes of this figure is the demonstration that the size of the localization region in the *z*-direction is close to, but slightly (by ~ 30%) smaller than, the radius of the tip for all the considered metals. This is an interesting observation that gives an immediate estimate of the typical localization region near the tip, which will be useful for practical applications of the considered nano-focusing structures. In particular, it is worth noting that such strong localization is not necessarily the conventional feature of all nano-focusing structures. For example, our estimates suggest that the field localization near the tip of a tapered wedge is significantly lower than for a tapered rod. This is a noticeable benefit of the tapered rod, which is related to significant differences in plasmon coupling in wedges and tapered rods.

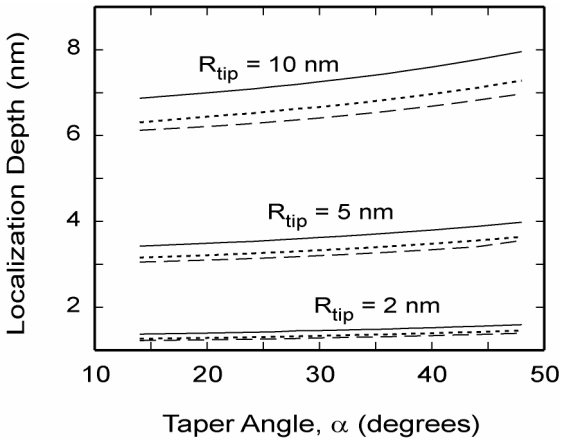

Fig. 8. Localization depth for the electric field, defined as the distance from the top of the rounded tip, such that at this distance the amplitude of the electric field decreases e times. The solid curves correspond to aluminum, the dotted curves correspond to silver, and the dashed curves correspond to gold.

It can also be seen that the localization depth slightly increases with increasing taper angle for all the considered metals (Fig. 8). However, this increase of the localization region does not seem to be strongly dependent upon taper angle, with the strongest dependence displayed for the largest radius of the tip (Fig. 8). In addition, increasing magnitude of the metal permittivity also results in some increase of the size of the localization region along the *z*-axis (compare the curves for different metals in Fig. 8). This is expected, because increasing metal permittivity typically results in larger portion of plasmon energy to be concentrated in the surrounding dielectric and increasing penetration depth into this dielectric.

It is somewhat counterintuitive that increasing magnitude of the metal permittivity simultaneously results in decreasing size the localization region along the surface of the rounded tip (Fig. 7). This however, should not be seen as a contradiction, because the localization region along the surface of the rounded tip is also dependent upon the actual process of reflection of the plasmon from the tip (i.e., on the features of the resultant standing wave pattern in the rod).

5 CONCLUSIONS

The results obtained in this paper have provided important practical information and criteria for fabrication and use of optimal nano-focusing structures based on plasmon propaga-

tion in tapered metal rods. In particular, we have confirmed the existence of optimal taper angle providing strong local electric field enhancement at the tip for a range of different metals (this angle was previously discussed in [14,26] for gold rods). We have demonstrated the existence of the optimal length of the tapered rod, which, in combination with the optimal taper angle, provides the maximal possible local field enhancement at the rounded tip of fixed radius of curvature. A simple analytical equation for the optimal rod length has been presented valid for a range of metals and plasmon frequencies, and verified against the rigorous numerical results. Three order of magnitude local field enhancements are shown to be achievable during plasmon nano-focusing in gold and especially silver nano-rods. Strong dependence of the local field enhancement on radius of curvature of the tip has also been demonstrated and investigated.

One of the important practical outcomes of this paper is that the optimal nano-focusing structures using metal rods are relatively large. For example, the optimal length for a gold rod is ~ 10 μm, while the optimal taper angle is ≈ 35°. For a silver tapered rod the optimal length is ~ 22 μm with the optimal taper angle ~ 30°, and for aluminum rod the optimal length is ~ 14 μm and the optimal taper angle ~ 20°. This means that the initial diameter of the tapered nano-focusing rod should be between ~ 4 μm and ~ 6 μm, in order to achieve maximal possible field enhancement at the tip. Such optimal tapered rods should be relatively easy to fabricate. Due to their geometrical parameters and dimensions, they should be strong and durable in use. Light could be relatively easily coupled into plasmons propagating in such rods (see, for example, [16]). Moreover, it has been shown that variations of rod length around the optimal length by up to ~ 50% do not result in significant variations of the resultant local field enhancement at the rounded tip. This demonstrates high tolerance of the described structures to fluctuations of rod length, and this seems to be highly beneficial for fabrication and practical use.

On the contrary, it has also been demonstrated that plasmon nano-focusing in all metal rods is highly sensitive to the conditions at the rounded tip. Therefore, it is important to accurate fabricate those rounded tips, with careful fabrication of their shape and dimensions. Proper fabrication of the rounded tip should ensure reproducible and strong local field enhancement of up to three orders of magnitude, which is very close to what is required for single molecule detection.

The comparison of the obtained numerical results with those from the adiabatic theory of nano-focusing has demonstrated the validity of the approximate theory in a relatively broad range of taper angles (up to ~ 35° for gold, ~ 30° for silver, and ~ 18° for aluminum), which opens wider opportunities for the successful use of the approximate and simplified adiabatic theory of nano-focusing in tapered metal rods [12,13]. We have also formulated a modified applicability condition for adiabatic theory for the analyses of plasmon propagation along cylindrical tapered structures for a range of different metals and plasmon frequencies. Corrections factors enabling use of the adiabatic theory for the evaluation of local field enhancement at the rounded tip of the tapered rod in the presence of plasmon reflections from the tip have been calculated and analyzed as functions of taper angle for all three considered metals.

Detailed investigation of the field structure near the rounded tip has revealed that the typical size of the region of localization of the plasmon field near the tip is of the order of, but slightly smaller (by ~ 30%) than, the radius of the rounded tip for the range of the considered metal tips. This gives an excellent understanding for the spatial scale for the plasmonic field near the tip, which will be important for practical applications of nano-focusing in the near-field microscopy and spectroscopy, optimal design of optical couplers for most effective delivery of the electromagnetic energy to nano-optical devices, quantum dots, single molecules, for the development of new optical sensors and measurement techniques (e.g., based on surface-enhanced Raman spectroscopy combined with nano-focusing), etc.

Acknowledgments

This work has been supported by the Australian Research Council (Linkage Grant LP0882614), Australian Federal Police Forensic Services, and National Institute of Forensic Sciences. The authors also acknowledge the support and technical help of the High Performance Computing Division at the Queensland University of Technology.

References

[1] D. W. Pohl, W. Denk, and M. Lanz, "Optical stethoscopy: Image recording with resolution λ/20," *Appl. Phys. Lett.* **44**, 651-653 (1984) [doi:10.1063/1.94865].

[2] L. Novotny and C. Hafner, "Light propagation in a cylindrical waveguide with a complex, metallic, dielectric function," *Phys Rev. E* **50**, 4094-4106 (1994) [doi:10.1103/PhysRevE.50.4094].

[3] L. Novotny, D. W. Pohl, and B. Hecht, "Light confinement in scanning near-field optical microscopy," *Ultramicroscopy* **61**, 1-9 (1995) [doi:10.1016/0304-3991(95)00095-X].

[4] S. Kawata, Ed., *Near-field Optics and Surface Plasmon-Polaritons*, Springer, Berlin (2001).

[5] A. Bouhelier, J. Renger, M. R. Beversluis, and L. Novotny, "Plasmon-coupled tip-enhanced near-field optical microscopy," *J. Microsc.* **210**, 220-224 (2003) [doi:10.1046/j.1365-2818.2003.01108.x].

[6] N. Anderson, A. Bouhelier, and L. Novotny, "Near-field photonics: tip-enhanced microscopy and spectroscopy on the nanoscale," *J. Opt. A* **8**, S227-S233 (2006) [doi:10.1088/1464-4258/8/4/S24].

[7] D. Mehtani, N. Lee, R. D. Hartschuh, A. Kisliuk, M. D. Foster, A. P. Sokolov, F. Cajko, and I. Tsukerman, "Optical properties and enhancement factors of the tips for apertureless near-field optics," *J. Opt. A* **8**, S183-S190(2006) [doi:10.1088/1464-4258/8/4/S19].

[8] K. V. Nerkararyan, T. Abrahamyan, E. Janunts, R. Khachatryan, and S. Harutyunyan, "Excitation and propagation of surface plasmon polaritons on the gold covered conical tip," *Phys. Lett. A* **350**, 147-149 (2006) [doi:10.1016/j.physleta.2005.09.072].

[9] K. Li, M. I. Stockman, and D. J. Bergman, "Self-similar chain of metal nanospheres as an efficient nanolens," *Phys. Rev. Lett.* **91**, 227402 (2003) [doi:10.1103/PhysRevLett.91.227402].

[10] K. Li, M. I. Stockman, and D. J. Bergman, "Enhanced second harmonic generation in a self-similar chain of metal nanospheres," *Phys. Rev. B* **72**, 153401 (2005) [doi:10.1103/PhysRevB.72.153401].

[11] A. J. Babadjanyan, N. L. Margaryan, and K. V. Nerkararyan, "Superfocusing of surface polaritons in the conical structure," *J. Appl. Phys.* **87**, 3785-3788 (2000) [doi:10.1063/1.372414].

[12] M. I. Stockman, "Nanofocusing of optical energy in tapered plasmonic waveguides," *Phys. Rev. Lett.* **93** 137404 (2004) [doi:10.1103/PhysRevLett.93.137404].

[13] M. W. Vogel and D. K. Gramotnev, "Adiabatic nano-focusing of plasmons by metallic tapered rods in the presence of dissipation," *Phys. Lett. A* **363**, 507–511 (2007) [doi:10.1016/j.physleta.2006.11.041].

[14] N. A. Issa and R. Guckenberger, "Optical nanofocusing on tapered metallic waveguides," *Plasmonics* **2**, 31-37 (2007) [doi: 10.1007/s11468-006-9022-7].

[15] N. A. Issa and R. Guckenberger, "Fluorescence near metal tips: the roles of energy transfer and surface plasmon polaritons," *Opt. Exp.* **15**, 12131-12144 (2007) [doi:10.1364/OE.15.012131].

[16] C. Ropers, C. C. Neacsu, T. Elsaesser, M. Albrecht, M. B. Raschke, and C. Lienau, "Grating-coupling of surface plasmons onto metallic tips: A nanoconfined light source," *Nano Lett.* **7**, 2784-2788 (2007) [doi:10.1021/nl071340m].
[17] D. K. Gramotnev, "Adiabatic nanofocusing of plasmons by sharp metallic grooves: Geometrical optics approach," *J. Appl. Phys.* **98**, 104302 (2005) [doi:10.1063/1.2130520].
[18] D. F. P. Pile and D. K. Gramotnev, "Adiabatic and nonadiabatic nanofocusing of plasmons by tapered gap plasmon waveguides," *Appl. Phys. Lett.* **89**, 041111 (2006) [doi:10.1063/1.2236219].
[19] D. K. Gramotnev and K. C. Vernon, "Adiabatic nano-focusing of plasmons by sharp metallic wedges," *Appl. Phys. B* **86**, 7-17 (2007) [doi:10.1007/S00340-006-2387-7].
[20] P. Ginzburg, D. Arbel, and M. Orenstein, "Gap plasmon polariton structure for very efficient microscale-to-nanoscale interfacing," *Opt. Lett.* **31**, 3288-3290 (2006) [doi:10.1364/OL.31.003288].
[21] D. K. Gramotnev, D. F. P. Pile, M. W. Vogel, and X. Zhang, "Local electric field enhancement during nanofocusing of plasmons by a tapered gap," *Phys. Rev. B* **75**, 035431 (2007) [doi:10.1103/PhysRevB.75.035431].
[22] K. C. Vernon, D. K. Gramotnev, and D. F. P. Pile, "Adiabatic nanofocusing of plasmons by a sharp metal wedge on a dielectric substrate," *J. Appl. Phys.* **101**, 104312 (2007) [doi:10.1063/1.2732699].
[23] M. Durach, A. Rusina, M. I. Stockman, and K. Nelson, "Toward full spatiotemporal control on the nanoscale," *Nano Lett.* **7**, 3145-3149 (2007) [doi:10.1021/nl071718g].
[24] E. Verhagen, L. Kuipers, and A. Polman, "Enhanced nonlinear optical effects with a tapered plasmonic waveguide," *Nano Lett.* **7**, 334-337 (2007) [doi:10.1021/nl062440f].
[25] E. D. Palik, *Handbook of Optical Constants of Solids*, Academic, New York (1985).
[26] D. K. Gramotnev, M. W. Vogel, and M. I. Stockman, "Optimized non-adiabatic nano-focusing of plasmons by tapered metal rods," *J. Appl. Phys.* **104**, 034311 (2008) [doi:10.1063/1.2963699].
[27] S. I. Bozhevolnyi, *Private communication and discussions*.